Research Square

Preprints are preliminary reports that have not undergone peer review.
They should not be considered conclusive, used to inform clinical practice,
or referenced by the media as validated information.

Theoretical Study on the Noncovalent Interactions Involving Triplet Diphenylcarbene

Chunhong Zhao
Hebei Normal University Huihua College
Hui Lin
Hebei Normal University
Aiting Shan
Hebei Normal University
Shaofu Guo
Hebei Normal University Huihua College
Xiaoyan Li
Hebei Normal University
Xueying Zhang (xueyingzhang@hebtu.edu.cn)
Hebei Normal University https://orcid.org/0000-0003-1598-8501

Research Article

Keywords: triplet diphenylcarbene, noncovalent interaction, electron density shift, electron spin density

Posted Date: May 19th, 2021

DOI: https://doi.org/10.21203/rs.3.rs-445417/v1

License: This work is licensed under a Creative Commons Attribution 4.0 International License.
Read Full License

Version of Record: A version of this preprint was published at Journal of Molecular Modeling on July 9th, 2021. See the published version at https://doi.org/10.1007/s00894-021-04838-6.

Abstract

The properties of some types of noncovalent interactions formed by triplet diphenylcarbene (DPC^3) have been investigated by means of density functional theory (DFT) calculations and quantum theory of atoms in molecules (QTAIM) studies. The $DPC^3\cdots LA$ (LA = AlF_3, SiF_4, PF_5, SF_2, ClF) complexes have been analyzed from their equilibrium geometries, binding energies, charge transfer and properties of electron density. The triel bond in the $DPC^3\cdots AlF_3$ complex exhibits a partially covalent nature, with the binding energy − 65.7kJ/mol. The tetrel bond, pnicogen bond, chalcogen bond and halogen bond in the $DPC^3\cdots LA$ (LA = SiF_4, PF_5, SF_2, ClF) complexes show the character of a weak closed-shell noncovalent interaction. Polarization plays an important role in the formation of the studied complexes. The strength of intermolecular interaction decreases in the order LA = AlF_3 > ClF > SF_2 > SiF_4 > PF_5. In the process of complexation, the charge transferrs from DPC^3 to the antibonding orbital of AlF_3/SF_2/ClF, the quantity of charge transfer is very small between DPC^3 and SiF_4/PF_5. The electron spin density transferrs from the radical DPC^3 to ClF and SF_2 in the formation of halogen bond and chalcogen bond, but for the $DPC^3\cdots AlF_3$/SiF_4/PF_5 complexes, the transfer of electron spin density is minimal.

1. Introduction

The study of noncovalent interactions has been a hot topic in supramolecular chemistry, molecular recognition and materials science [1]. The strength of noncovalent bonds is smaller than general chemical bonds about 1 ~ 2 orders of magnitude, but in the system containing large numbers of molecules, the noncovalent interactions accumulate and influence the structure, function, physical and chemical properties of the system. Of the various noncovalent bonds, hydrogen bond and halogen bond are arguably the most important and prevalent [2–5]. Hydrogen bond is typically expressed as the positioning of two molecules such that the H atom of one molecule, R − H, acts as a bridge to another molecule R − H···D. The anisotropic charge distribution around atom of Groups 12–18 allows them to act in a similar capacity. The concepts of σ-holes or π-holes that have been pointed out by Politzer and Clark et al. [6–12] reflect the fact that covalently-bonded atom tends to have anisotropic electronic densities, with regions of higher and lower density. A σ-hole or π-hole is a region of lower electronic density along the extension of a covalently-bonded atom, or perpendicular to a planar portion of a molecule. This region gives rise to positive electrostatic potential, can be used as a Lewis acid to interact attractively with the rich electronic center (lone pairs, π electrons, anions, etc.) of a Lewis base. One or more σ-holes or π-holes has been found for all of the main-group elements in the Periodic Table and has been classified into a wide variety of noncovalent interactions: alkaline earth bonds for Group 12, triel bonds for Group 13, tetrel bonds for Group 14, pnicogen bonds for Group 15, chalcogen bonds for Group 16, halogen bonds for Group17, and aerogen bonds for Group 18 [4, 5, 13–22]. Recently, noncovalent interactions involving σ-hole or σ-lump on a coinage metal have been reported [23–25].

As organic reactive intermediates containing two unbonding valence electrons on a divalent carbon atom, carbenes can activate small molecules under mild conditions, catalyze organic reactions, and act as ligands in transition metal catalysis [26]. Depending on whether two electrons in carbon atom of carbene are located in a same or a different orbital, they give place to a singlet or a triplet configuration, respectively. Because of its lone pairs, singlet carbenes can be acted as electron-pair donors in the intermolecular interactions. Del Bene and Alkorta et al. [27–30] studied a series of carbenes and silyenes as hydrogen and pnicogen bond acceptors, they also shown that nitrogen heterocyclic carbenes (NHCs) might prefer noncovalent or covalent bonding to trap CO_2 and CS_2. Some carbene lithium bonding, triel bonding, tetrel bonding and pnicogen bonding interactions were predicted and characterized by theoretical calculations [31–35]. Sander et al. [36–38] investigated the interactions between diphenylcarbene (DPC) and H_2O, CH_3OH, or CF_3I using matrix isolation spectroscopy (IR, UV-vis and EPR) in combination with theoretical calculations. They showed that the spin ground state of DPC switches from triplet to singlet upon formation of the strongly hydrogen-bonded and halogen-bonded complexes. Lu et al. [39] further discussed the influence of the formation of halogen bond on the spin state of DPC and the decisive factors in spin slip via density functional theory (DFT) calculations.

In view of the fact that diphenylcarbene is a prototypical transient carbene with a triplet ground state and has been subject to a large number of mechanistic studies using time-resolved or low-temperature spectroscopy, the bimolecular complexes between triplet diphenylcarbene (DPC^3) and a series of Lewis acids LA (LA = AlF_3 SiF_4, PF_5, SF_2, ClF) from Group 13–17 atoms were constructed in this work, in order to give insight into these kinds of noncovalent interactions. The main purposes of this paper are: (1) to study the stability and strength of the complexes containing triplet DPC^3; (2) to investigate the character of these σ/π-hole interactions; (3) to analyze the influence of noncovalent interaction on the distribution of electron density and electron spin density.

2. Computational Methods

All calculations were performed with Gaussian 09 program package [40]. The geometries of the monomers and complexes were fully optimized using the B3LYP functional with D3 empirical dispersion correction and 6-311 + + G** basis set. Harmonic frequencies were calculated to confirm the equilibrium geometries to be true minima and yielded zero-point energy. The keyword Counterpoise was used for the calculation of corrected binding energies, excluding the inherent basis set superposition error (BSSE) [41]. The binding energies of the bimolecular complexes were computed as the difference between the energy of the complex and the sum of energies of corresponding isolated monomers, in which the geometries of monomers were optimized solely. The electrostatic potentials were calculated on the 0.001 a.u. (electrons/$Bohr^3$) contour of the electron density of the molecule with the WFA surface analysis suite [42]. The natural bond orbital (NBO) method was used to obtain the stabilizing charge-transfer interactions for the complexes using the NBO6.0 program [43]. To have a more detailed and in-depth understanding of the interactions, topological properties of the electron density at the bond critical points were computed

by the AIMAll program [44]. Noncovalent interaction index (NCI) and electron spin density analysis were carried out using Multiwfn software [45], and the related plots were graphed using theVMD program [46].

3. Results And Discussion

3.1 Molecular electrostatic potentials

Molecular electrostatic potential (MEP) is a fundamentally important physical characteristic that very useful for understanding and predicting noncovalent interactions. Figure 1 shows the contour maps of MEPs for triplet biphenyclobin (DPC^3) and LA (LA = AlF_3, SiF_4, PF_5, SF_2, ClF). The most positive electrostatic potentials ($V_{S,max}$) and most negative electrostatic potentials ($V_{S,min}$) on the 0.001 au contour of the molecular electron density are collected in Table 1. As shown in Fig. 1a, the contour map for DPC^3 presents a few blue regions with negative MEPs. The positions of $V_{S,min}$ are located above and below the benzene ring, represented by blue dots, with the values of -13.7 and − 12.2 kcal/mol, respectively. From the contour map of MEP for AlF_3 (Fig. 1b), aluminum atom acts as the Lewis acid center since it is characterized by the depletion of electron charge (π-hole) [7, 14]. This red region corresponds to the vacant p orbital perpendicular to the plane of AlF_3 molecular framework, with a $V_{S,max}$ value of 104.7 kcal/mol. In the case of ClF, SF_2, SiF_4 and PF_5, there are one or more σ-holes (red regions) with positive MEPs along the extension of the corresponding Cl-F, S-F, Si-F and P-F bond. The $V_{S,max}$ values were found to become increasingly more positive following the order $AlF_3 > SiF_4 > ClF > SF_2 > PF_5$.

Table 1
Most positive and negative MEPs of the monomers ($V_{S,max}$, $V_{S,min}$ in kcal/mol)

Molecule	$V_{S,min}$	$V_{S,max}$
DPC^3	-13.7/-12.2	-
AlF_3	-	104.7
SiF_4	-	47.4
PF_5	-	39.9
SF_2	-	41.4
ClF	-	44.6

3.2 Geometry, binding energy and NBO analysis

Based on the analysis of MEPs, the intermolecular interaction could form between the σ-hole or π-hole regions of LA (LA = AlF_3, SiF_4, PF_5, SF_2, ClF) and the negative electrostatic potential region of DPC^3.

Figure 2 shows the stable geometries of DPC^3···LA (LA = AlF_3, SiF_4, PF_5, SF_2, ClF) complexes. It can be seen that the most stable interaction between DPC^3 and LA (LA = AlF_3, SiF_4, PF_5, SF_2, ClF) occurs on the benzene ring of DPC^3. The binding energy, binding distance and the main parameters of NBO analysis for the complexes are given in Table 2. The binding energy (ΔE) ranges from − 15.8 kJ/mol for pnicogen-bonded complex DPC^3···PF_5 to -65.7 kJ/mol for triel-bonded complexes DPC^3···AlF_3. The strength of intermolecular interaction become stronger along the sequence LA = PF_5 < SiF_4 < SF_2 < ClF < AlF_3. Binding distance (d) in the Table 2 refers to the distance between the atom of Group 13 to 17 in the LA (LA = AlF_3, SiF_4, PF_5, SF_2, ClF) and the nearest carbon atom of benzene ring in DPC^3, which can be seen that the shorter the binding distance, the stronger the interaction. By comparing the data in Table 1 and Table 2, it is found that the binding energy between molecules is not well correlated with the $V_{S,max}$ values of Lewis acids, which may be due to the steric hindrance effect of SiF_4 and PF_5.

Table 2
Binding energy, binding distance, and main parameters of NBO and MFDD analyses for the complexes DPC^3···LA (LA = AlF_3, SiF_4 PF_5, SF_2, ClF) (energy in kJ/mol, distance in Å, charge in e)

Complex	ΔE	d	Donor NBO	Acceptor NBO	$E^{(2)}$	Q_{CT}	Δn_e
DPC^3···AlF_3	-65.7	2.368	BD(C-C)	LV(Al)	12.43	0.1078	0.1897
			3C(C-C-C)	LV(Al)	17.95		
DPC^3···SiF_4	-19.7	3.669	LP(F)	BD*(C-H)	0.88	-0.0045	0.0266
DPC^3···PF_5	-15.8	3.669	LP(F)	BD*(C-H)	0.84	-0.0027	0.0280
DPC^3···SF_2	-20.5	3.183	BD(C-C)	BD*(S-F)	4.43	0.0212	0.0378
DPC^3···ClF	-30.1	2.651	BD(C-C)	BD*(Cl-F)	113.55	0.1690	0.0554

For a better understanding of orbital interaction and charge transfer between specific orbitals of each monomer, NBO analysis was performed at the B3LYP-D3/6-311 + + G** level. The lump sum of the charge transferred between the molecules is reported as Q_{CT} in the last column of Table 2. The values of Q_{CT} for the complexes DPC^3···LA (LA = AlF_3, SiF_4, PF_5, SF_2, ClF) are 0.1078e, -0.0045e, -0.0027e, 0.0212e and 0.1690e, respectively. The positive CT quantities indicate that charge is transferred from DPC^3 to AlF_3, SF_2 or ClF, as would be expected for triel bond, chalcogen bond and halogen bond. For the complexes formed by SiF_4 and PF_5, the charge transfer is very small and negative, reflecting the fact that little net charge is apparently transferred from SiF_4/PF_5 to DPC^3; this may be the cause of steric crowding in tetrel bond and pnicogen bond. The tetravalent/pentavalent character of Si/P atom leaves only limited room for an incoming nucleophile to approach and engage in a noncovalent bond with a tetrel/phosphorus atom [47]. The charge transfer occurs mainly from the F lone pairs in SiF_4/PF_5 to the C-H antibonding orbital in the DPC^3, with small second order perturbation energy ($E^{(2)}$) 0.88 kJ/mol and 0.84 kJ/mol,

respectively. From Table 2, the strongest orbital interaction is happened in the halogen-bonded complex DPC^3···ClF. The $E^{(2)}$ value between the C-C bonding orbital (BD(C-C)) and antibonding Cl-F orbital (BD*(Cl-F)) was calculated to be 113.6 kJ/mol. In the triel-bonded complex DPC^3···AlF_3, the main electron transfer is from the C-C bond orbital (BD(C-C)) and 3-center bonding orbital (3C(C-C-C)) in the DPC^3 to the lone vacancy of aluminum atom (LV(Al)) in the AlF_3. For chalcogen-bonded complex DPC^3···SF_2, charge transfer occurs from the C-C bonding orbital in the DPC^3 to the S-F antibonding orbital in the SF_2 (BD(C-C) → BD*(S-F)), $E^{(2)}$ and CT were calculated to be 4.43 kJ/mol and 0.0212e .

3.3 Noncovalent interaction index

To verify the intermolecular interaction between DPC^3 and LA (LA = AlF_3, SiF_4, PF_5, SF_2, ClF), the complexes were analyzed by noncovalent interaction index (NCI). This method, proposed by Yang's research group [48, 49], can not only describe the properties of the interacting molecules, but also show the characteristic information of the interaction through graphics. Based on the analysis of the electron density (ρ) and its reduced density gradient function (RDG), this approach combines with the electron density and sign(λ_2) to analyze the type and strength of interactions between molecules, where sign(λ_2) is the sign of the second eigenvalue of its Hessian. In the isosurface of the reduced density gradient function, blue represents strong attractive interaction, green represents weak interaction, and red indicates strong nonbonded overlap, such as steric effect in a ring or cage. Figure 3 shows the plots of the reduced density gradient versus the electron density multiplied by sign(λ_2) (above) and gradient isosurfaces generated for s = 0.05 au (below). In the DPC^3 complexes, several low-density isosurfaces (green regions) lie in the interacting portions between DPC^3 and LA (LA = AlF_3, SiF_4, PF_5, SF_2, ClF), where noncovalent attractions are expected. There is another area of the low-density, low-gradient nonbonded overlap (red region) located at the center of each benzene ring, where steric repulsion in the benzene ring. For the triel-bonded complex, the blue isosurface lies between the π-hole of AlF_3 and benzene ring of DPC^3, reveals stronger interaction than in the other complexes. The locations of ρ(r) peaks for the complexes DPC^3···LA (LA = AlF_3, SiF_4, PF_5, SF_2, ClF) are consistent with the interaction strengths.

3.4 QTAIM analysis

Based on the quantum theory of atoms in molecules (QTAIM) [50, 51], the molecular structures, the characters of chemical bonds and chemical reactions are closely related to the electron density distribution functions. The strength and properties of a chemical bond can be determined through the relative parameters of the electron density and the energy density at the critical points in molecules [52–54]. The common studied topological properties at the bond critical points (BCPs) are electron density (ρ_b), its Laplacian ($\nabla^2\rho_b$), the local potential energy density (V_b), local kinetic energy density (G_b), and total energy density ($H_b = V_b + G_b$). According to criteria [55, 56], a positive $\nabla^2\rho_b$ reflects an excess of kinetic energy in bonds and a relative depletion of electronic charge along a bond path. A positive H_b corresponds to a purely closed-shell interaction, whereas a negative H_b value corresponds to bonds with any degree of covalent character. If $-G_b/V_b$ is greater than 1, then the interaction is noncovalent. If the

ratio is between 0.5 and 1, the interaction is partly covalent in nature, and when this ratio is less than 0.5, the interaction is a shared covalent one.

The molecular graphs and the topological properties of electron density at the BCPs of the complexes are showed in Fig. 4 and Table 3. For $DPC^3 \cdots AlF_3$ complex, there exists a BCP between the π-hole of AlF_3 and C atom of DPC^3, and a pair of bond paths connect the BCP and the interacting Al and C atom. The values of ρ_b and $\nabla^2\rho_b$ at the C···Al BCP were calculated to be 0.0296 au and 0.0710 au. Positive $\nabla^2\rho_b$ value, negative H_b value, and $-G_b/V$ value of about 0.8 indicate that this triel bond is of moderate strength with a partially covalent nature. For complex $DPC^3 \cdots SiF_4$ and $DPC^3 \cdots PF_5$, there exist several C···F BCPs and one H···F BCP between DPC^3 and SiF_4/PF_5 molecules, the ρ_b values are less than 0.0090 au. From Fig. 4d and 4e, the C···S or C···Cl BCP in the $DPC^3 \cdots SF_2$ and $DPC^3 \cdots ClF$ complexes account for the chalcogen bond or pnicogen bond between DPC^3 and σ-hole of SF_2/ClF. The ρ_b and $\nabla^2\rho_b$ values of the complexes $DPC^3 \cdots LA$ (LA = SiF_4, PF_5, SF_2, ClF) are in the range of 0.0044 ~ 0.0296 au and 0.0155 ~ 0.0621 au. $\nabla^2\rho_b > 0$, $H_b > 0$ and $-G_b/V_b > 1$ were calculated, showing the characters of a weak closed-shell noncovalent interaction.

Table 3
Topological properties of electron density at the bond critical points for the complexes $DPC^3 \cdots LA$ (LA = AlF_3, SiF_4 PF_5, SF_2, ClF) (in au)

Complex	BCP	ρ_b	$\nabla^2\rho_b$	G_b	V_b	H_b	$-G_b/V_b$
$DPC^3 \cdots AlF_3$	C···Al	0.0296	0.0710	0.0230	-0.0283	-0.0053	0.8132
	H···H	0.0063	0.0247	0.0048	-0.0035	0.0013	1.3788
	H···F	0.0094	0.0332	0.0072	-0.0062	0.0011	1.1734
$DPC^3 \cdots SiF_4$	C···F	0.0052	0.0194	0.0040	-0.0031	0.0009	1.2868
	C···F	0.0052	0.0195	0.0040	-0.0030	0.0009	1.3056
	C···F	0.0044	0.0155	0.0031	-0.0024	0.0008	1.3178
	H···F	0.0081	0.0306	0.0066	-0.0056	0.0010	1.1853
$DPC^3 \cdots PF_5$	H···F	0.0090	0.0338	0.0073	-0.0061	0.0012	1.1907
	C···F	0.0061	0.0251	0.0052	-0.0041	0.0010	1.2623
	C···F	0.0066	0.0244	0.0051	-0.0042	0.0010	1.2352
$DPC^3 \cdots SF_2$	C···S	0.0102	0.0292	0.0062	-0.0051	0.0011	1.2219
	H···F	0.0080	0.0303	0.0065	-0.0055	0.0010	1.1841
$DPC^3 \cdots ClF$	C···Cl	0.0258	0.0621	0.1512	-0.0149	0.0003	1.0219

3.5 Density difference of molecular formation analysis

The density difference during the formation of super molecules (A···B) can be described as $\rho_d(r) = \rho_{complex}(r) - (\rho_{molA}(r) + \rho_{molB}(r))$. According to Politzer et al. [57], polarization is a real physical phenomenon, corresponding to the electron density shifts from one molecule to the electric field of another, could be observed physically from the electronic density. Density difference of molecular formation (MFDD) analysis has often been used to study the formation of molecules and weak interactions [58–60]. Figure 5 present plots of computed density difference of the complexes, the shift of charge density during the forming of DPC^3···LA (LA = AlF_3, SiF_4, PF_5, SF_2, ClF) complexes are clearly shown. The electronic fields of the π electrons in DPC^3 and σ/π-hole in LA cause charge redistributions of each segment. From Fig. 5a and 5e, one can see a few negative regions (blue regions) outside the carbon atoms and Al/Cl atom, which means that a decrease in electron density when DPC^3 and LA interact to form the complexes. An increased region in electron density (white region) between the carbon atoms and Al/Cl atom could be found during the formation of the triel bond and halogen bond. From AlF_3, ClF to SF_2, SiF_4 and PF_5, the degree of charge density in the intermolecular region becomes more and more slight. We chose this increased region as a cube to integrate the total charge of the density difference, the positive integral charge (Δn_e) were obtained and shown in the last column of Table 2. Linear correlation was found between the integral charges and the binding energies, with the correlation coefficients 0.982 (Fig. 6). The stronger DPC^3···LA interaction increases the electric field in the intermolecular region, resulting in a larger increase in electron density between molecules. These results indicate that polarization effect plays an important role when DPC^3 interact with Lewis acids.

3.6 Electron spin density analysis

For open shell system, total electron density is the sum of α and β electron densities, i.e., $\rho(\text{total}) = \rho(\alpha) + \rho(\beta)$. The difference between $\rho(\alpha)$ and $\rho(\beta)$, $\Delta\rho = \rho(\alpha) - \rho(\beta)$, represents the electron spin density of the system. The value $\Delta\rho$ is equal to 0 and 2 in the LA and triplet DPC^3 molecules. Figure 7 show the maps of electron spin density of DPC^3 and its complexes DPC^3···ClF and DPC^3···SF_2, the $\Delta\rho$ values of C atoms in DPC^3 are marked out. Green regions represent positive and blue regions represent negative $\Delta\rho$ values. To illustrate the electron spin density transfer during bond formation, Table 4 lists the electron spin density changes of C atoms and LA in the formation of the complexes.

Table 4
Changes of electron spin density for carbon atoms and LA in the complexes (in au)

Complex	$DPC^3\cdots AlF_3$	$DPC^3\cdots SiF_4$	$DPC^3\cdots PF_5$	$DPC^3\cdots SF_2$	$DPC^3\cdots ClF$
$\Delta\Delta\rho$(C1)	0.0028	0.0087	0.0087	-0.0004	-0.0550
$\Delta\Delta\rho$(C2)	0.0077	0.0003	0.0016	-0.0001	0.0052
$\Delta\Delta\rho$(C3)	-0.0095	0.0032	0.0003	-0.0008	-0.0100
$\Delta\Delta\rho$(C4)	-0.0130	0.0010	-0.0017	-0.0015	-0.0097
$\Delta\Delta\rho$(C5)	0.0047	-0.0007	0.0004	0.0004	0.0036
$\Delta\Delta\rho$(C7)	0.0051	-0.0007	0.0004	0.0003	0.0035
$\Delta\Delta\rho$(C9)	-0.0128	0.0024	-0.0009	-0.0019	-0.0101
$\Delta\Delta\rho$(C13)	0.0160	0.0061	0.0051	0.0076	0.0089
$\Delta\Delta\rho$(C14)	-0.0021	-0.0138	-0.0097	-0.0126	-0.0516
$\Delta\Delta\rho$(C15)	-0.0235	-0.0070	-0.0052	-0.0083	-0.0029
$\Delta\Delta\rho$(C16)	0.0094	0.0050	0.0039	0.0068	0.0219
$\Delta\Delta\rho$(C18)	0.0203	0.0043	0.0041	0.0058	0.0087
$\Delta\Delta\rho$(C20)	-00056	-0.0103	-0.0077	-0.0107	-0.0126
$\Delta\Delta\rho$(LA)	-0.0004	0.0009	0.0002	0.0143	0.0980

The calculated results show that the electron spin density is primarily concentrated on the divalent C1 atom of DPC^3, the $\Delta\rho$ value of C1 is 1.4038e in the monomer. In the process of formation of the complexes, there is a rearrangement of electron spin density. For the complexes $DPC^3\cdots$LA (LA = AlF_3, SiF_4, PF_5), the sum of spin electron densities in LA is less than 0.0009. These values are too small to be significant, indicating that spin density rearranges within the DPC^3 radicals, and the transfer of spin electron density from the electron donor to acceptor can be ignored. In $DPC^3\cdots AlF_3$ complex, the change of spin electron density occurs mainly in C15 and C18 atoms of DPC^3. In $DPC^3\cdots SiF_4/PF_5$ complexes, the change of spin electron density occurs mainly in C1, C14 and C20 atoms. In the process of chalcogen bond formation, the electron spin densities of the C14 and C20 atoms decrease and those of the S and F atoms increase; the sum of spin electron densities in SF_2 is 0.0143. For the halogen-bonded complex DPC^3…ClF, the changes of electron spin density in C1 and C14 atoms are − 0.0550 and − 0.0516, meanwhile, the sum of electron spin density in ClF is 0.0980. The increased values of SF_2/ClF indicate that a quantity of electron spin density transfer from DPC^3 to SF_2/ClF.

Therefore, in the process of the formation of $DPC^3\cdots$LA (LA = AlF_3, SiF_4, PF_5) complexes, the transfers of the electron spin density from DPC^3 to LA is minimal, but it rearranges within the radical itself. For the

chalcogen-bonded and halogen-bonded complex, certain electron spin density transfer from the radical to Lewis acid.

4 Conclusions

In this work, the intermolecular interactions between the triplet biphenylcarbene radical DPC^3 and a series of Lewis acids LA (LA = AlF_3, SiF_4, PF_5, SF_2 and ClF) have been investigated. The analyses of NCI, AIM, and MFDD et al. generated the following conclusions:

(1) The strength of intermolecular interaction between DPC^3 and a series of Lewis acids LA decreases gradually in the order of LA = AlF_3 > ClF > SF_2 > SiF_4 > PF_5. The triel bond in the $DPC^3\cdots AlF_3$ complex is of moderate strength and partially covalent nature. Other intermolecular interactions between DPC^3 and LA (LA = SiF_4, PF_5, SF_2 and ClF) are characterized by weak closed-shell noncovalent interactions.

(2) The intermolecular interaction induces a build-up of electric charge between molecules. The integral value of the positive charge of density difference is consistent with the binding energy, and polarization effect plays an important role.

(3) In the process of halogen bond and chalcogen bond formation, the electron spin density is transferred from DPC^3 to ClF and SF_2, while during the interaction of DPC^3 with AlF_3, SiF_4 and PF_5, the transfer of electron spin density between molecules is negligible, the electron spin density rearrange within the radical itself.

Declarations

Authors' contributions Chunhong Zhao: investigation, writing—original draft; Hui Lin: formal analysis, data curation; Aiting Shan: visualization; Shaofu Guo: writing—review and editing; Xiaoyan Li: methodology, supervision; Xueying Zhang: conceptualization, supervision.

Funding This work was supported by National Natural Science Foundation of China (Contract No. 21973027 of Prof. Xiaoyan Li), Natural Science Foundation of Hebei Province (Contract No. B2020205002 of Prof. Xiaoyan Li), and the Foundation of Hebei Normal University (Contract No. L2018Z04 of Dr. Xueying Zhang).

Data availability The manuscript has full control of all primary data, and the authors agree to allow the journal to review their data if requested.

Code availability N/A

Compliance with ethical standards

Conflict of interest The authors declare that they have no competing interests.

Consent for publication Written informed consent for publication was obtained from all participants.

References

1. Müller-Dethlefs K, Hobza P (2000) Noncovalent interactions: a challenge for experiment and theory. Chem Rev 100:143-168.
2. Gilli G, Gilli P (2009) The nature of the hydrogen bond: outline of a comprehensive hydrogen bond theory. Oxford University Press.
3. Scheiner S (2019) Forty years of progress in the study of the hydrogen bond. Struct Chem 30:1119–1128.
4. Metrangolo P, Neukirch H, Pilati T, Resnati G (2005) Halogen bonding based recognition processes: a world parallel to hydrogen bonding. Acc Chem Res 38: 386-395.
5. Wang H, Wang W, Jin WJ (2016) σ-Hole bond vs π-hole bond: a comparison based on halogen bond. Chem Rev 116:5072-104.
6. Clark T, Hennemann M, Murray JS, Politzer P (2007) Halogen bonding: the σ-hole. J Mol Model 13:291-296.
7. Murray JS, Lane P, Clark T, Riley KE, Politzer P (2012) σ-Holes, π-holes and electrostatically-driven interactions. J Mol Model 18:541-548.
8. Politzer P, Murray JS (2013) Halogen bonding: an interim discussion. ChemPhysChem 14:278–294.
9. Politzer P, Murray JS, Clark T (2013) Halogen bonding and other σ-hole interactions: a perspective. Phys Chem Chem Phys 15:11178-11189.
10. Politzer P, Murray, JS, Clark T, Resnati G (2017) The σ-hole revisited. Phys Chem Chem Phys 19: 32166-32178.
11. Politzer P, Murray JS (2019) An overview of strengths and directionalities of noncovalent interactions: σ-holes and π-holes. Crystals 9: 165
12. Politzer P, Murray JS (2020) Electrostatics and polarization in σ- and π-hole noncovalent interactions: an overview. ChemPhysChem 21: 579–588
13. Yáñez M, Sanz P, Mó O, Alkorta I, Elguero J (2009) Beryllium bonds, do they exist? J Chem Theor Comput 5:2763–2771.
14. Grabowski SJ (2014) Boron and other triel Lewis acid centers: from hypovalency to hypervalency. ChemPhysChem 15(14):2985-2993.
15. Gao L, Zeng Y, Zhang X, Meng L (2016) Comparative studies on group III σ-hole and π-hole interactions. J Comput Chem 37, 14: 1321-1327
16. Bauzá A, Mooibroek TJ, Frontera A (2013) Tetrel-bonding interaction: rediscovered supramolecular force? Angew Chem Int Ed 52(47):12317-12321.
17. Zahn S, FrankR, Hey-HawkinsE, KirchnerB (2011) Pnicogen bonds: a new molecular linker? Chem Eur J 17(22):6034-6038.

18. Wang W, Ji B, Zhang Y (2009) Chalcogen bond: a sister noncovalent bond to halogen bond. J Phys Chem A 113:8132–8135.
19. Cavallo G, Metrangolo P, Milani R, Pilati T, Priimagi A, Resnati G, Terraneo G (2016) The halogen bond. Chem Rev 116:2478–2601.
20. Bauzá, A, Frontera A (2015) Aerogen bonding interaction: a new supramolecular force? Angew Chem Int Ed 54:7340–7343.
21. Cavallo G, Metrangolo P, Pilati T, Resnati G, Terraneo G. (2014) Naming interactions from the electrophilic site. Cryst Growth Des 14:2697–2702
22. Legon AC (2017) Tetrel, pnictogen and chalcogen bonds identified in the gas phase before they had names: a systematic look at non-covalent interactions. Phys Chem Chem Phys 19(23):14884-14896
23. Legon AC, Walker NR (2018) What's in a name? 'Coinage-metal' non-covalent bonds and their definition. Phys Chem Chem Phys 20:19332-19338
24. Cui J, Zhang X, Meng L, Li Q, Zeng Y (2019) Coinage metal dimers as the noncovalent interaction acceptors: study of the σ-lump interactions. Phys Chem Chem Phys 21:21152-21161
25. Zheng B, Liu Y, Wang Z, Zhou F, Jiao Y, Liu Y, Ding X, Li Q (2018) Comparison of halide donators based on pi···M (M=Cu, Ag, Au), pi···H and pi···halogen bonds. Theor Chem Acc 137:179
26. Moss RA, Doyle MP (2014) Contemporary carbene chemistry. Wiley, Hoboken
27. Alkorta I, Elguero J (1996) Carbenes and silylenes as hydrogen bond acceptors. J Phys Chem 100:19367-71930
28. Del Bene JE, Alkorta I, Elguero J (2017) Carbenes as electron-pair donors for P···C pnicogen bonds. ChemPhysChem 18(12):1597-1610.
29. Alkorta I, Montero-Campillo MM, Elguero J (2017) Trapping CO_2 by adduct formation with nitrogen heterocyclic carbenes (NHCs): a theoretical study. Chem-Eur J 23(44):10604-10609
30. Del Bene JE, Alkorta I, Elguero J (2017) Carbon–carbon bonding between nitrogen heterocyclic carbenes and CO_2. J Phys Chem A 121(42):8136-8146
31. Li Q, Wang H, Liu Z, Li W, Sun J (2009) Ab initio study of lithium-bonded complexes with carbene as an electron donor. J Phys Chem A 113(51):14156-14160
32. Zhuo H, Li Q (2015) Novel pnicogen bonding interactions with silylene as an electron donor: covalency, unusual substituent effects and new mechanisms. Phys Chem Chem Phys 17(14):9153-9160
33. Liu M, Li Q, Li W, Cheng J (2017) Carbene tetrel-bonded complexes. Struct Chem 28(3):823-831
34. Chi Z, Dong W, Li Q, Yang X, Scheiner S, Liu S (2019) Carbene triel bonds between TrR_3 (Tr = B, Al) and N-heterocyclic carbenes. Int J Quantum Chem 119(8):e25867
35. Lin H, Meng L, Li X, Zeng Y, Zhang X (2019) Comparison of pnicogen and tetrel bonds in complexes containing CX_2 carbenes (X = F, Cl, Br, OH, OMe, NH_2, and NMe_2). New J Chem 43:15596-15604
36. Costa P, Fernandez-Oliva M, Sanchez-Garcia E, Sander W (2014) The highly reactive benzhydryl cation isolated and stabilized in water ice. J Am Chem Soc 136: 15625–15630

37. Costa P, Sander W (2014) Hydrogen bonding switches the spin state of diphenylcarbene from triplet to singlet. Angew Chem Int Ed 53:5122–5125
38. Henkel S, Costa P, Klute L, Sokkar P, Fernandez-Oliva M, Thiel W, Sanchez-Garcia E, Sander W (2016) Switching the spin state of diphenylcarbene via halogen bonding. J Am Chem Soc 138(5):1689-1697.
39. Ge Y, Lu Y, Xu Z, Liu H (2018) Controlling the spin state of diphenylcarbene via halogen bonding: a theoretical study. Int J Quantum Chem 118(15): e25616.
40. Frisch MJ, Trucks GW, Schlegel HB, Scuseria GE, Ma R, Cheeseman JR, Scamani G, Barone V, Mennucci B, Petersson GA, Nakatsuji H, Caricato M, Li X, Hratchian HP, Izmaylov AF, BloinoJ ZG, Sonnenberg JL, Hada M, Ehara M, Toyota K, Fukuda R, Hasegawa J, Ishida M, Nakajima T, Honda Y, Kitao O, Nakai H, Vreven T, Montgomery Jr JA, Peralta JE, Ogliaro F, Bearpark M, Heyd JJ, Brothers E, Kudin KN, Staroverov VN, Keith T, Kobayashi R, Normand J, Raghavachari K, Rendell A, Burant JC, Iyengar SS, Tomasi J, Cossi M, Rega N, Millam JM, Klene M, Knox JE, Cross JB, Bakken V, Adamo C, Jaramillo J, Gomperts R, Stratmann RE, Yazyev O, Austin AJ, Cammi R, Pomelli C,Ochterski JW, Martin RL, Morokuma K, Zakrzewski VG, Voth GA, Salvador P,Dannenberg JJ, Dapprich S, Daniels AD, Farkas O, Foresman JB, Ortiz JV, Cioslowski J, Fox DJ (2013) Gaussian09. Gaussian Inc., Wallingford
41. Boys SF, Bernardi F (1970) The calculation of small molecular interactions by the differences of separate total energies. some procedures with reduced errors. Mol Phys 19(4):553-566
42. Bulat FA, Toro-Labbé A, Brinck T, Murray JS, Politzer P (2010) Quantitative analysis of molecular surfaces: areas, volumes, electrostatic potentials and average local ionization energies. J Mol Model 16(11):1679-1691
43. Glendening ED, Landis CR, Weinhold F. (2013) NBO 6.0: Natural bond orbital analysis program. J Comput Chem 34(16):1429-1437
44. Keith TA. (2015) Computational improvements for the theory of atoms in molecules. AIMAll (Version 15.09.27), TK Gristmill Software, Overland Park KS, USA
45. Lu T, Chen F (2012) Multiwfn: a multifunctional wavefunction analyzer. J Comput Chem 33(5):580-592
46. Humphrey W, Dalke A, Schulten K. (1996) VMD: visual molecular dynamics. J Mol Graph 14(1):33-38
47. Scheiner S, (2018) Steric Crowding in Tetrel Bonds. J Phys Chem A 122:2550-2562
48. Johnson ER, Keinan S, Mori-Sanchez P, Contreras-Garcia J, Cohen AJ, Yang W (2010) Revealing Noncovalent Interactions. J Am Chem Soc 132(18):6498-6506
49. Contreras-Garcia J, Johnson ER, Keinan S, Chaudret R, Piquemal JP, Beratan DN, Yang W (2011) NCIPLOT: a program for plotting noncovalent interaction regions. J Chem Theory Comput 7(3):625–632
50. Bader RFW (1991) A quantum theory of molecular structure and its applications. Chem Rev 91(5):893–928
51. Becke A, Matta CF, Boyd RJ (2007) The quantum theory of atoms in molecules. Wiley, New York.

52. Zeng Y, Zhang X, Li X, Meng L, Zheng S (2011) The role of molecular electrostatic potentials in the formation of a halogen bond in Furan···XY and Thiophene···XY complexes. ChemPhysChem 12:1080-1087
53. Rozas I, Alkorta I, Elguero J (2000) Behavior of ylides containing N, O, and C atoms as hydrogen bond acceptors. J Am Chem Soc 122:11154-11161
54. Grabowski SJ (2012) QTAIM characteristics of halogen bond and related interactions. J Phy Chem A 116:1838−1845
55. Cremer D, Kraka E (1984) Chemical bonds without bonding electron density — Does the difference electron-density analysis suffice for a description of the chemical bond? Angew Chem Int Ed 23(23):627–628;
56. Bone RGA, Bader RFW (1996) Identifying and analyzing intermolecular bonding interactions in van der Waals molecules. J Phys Chem 100(26):10892-10911
57. Politzer P, Murray JS, Clark T (2015) Mathematical modeling and physical reality in noncovalent interactions. J Mol Model 21:52
58. Zheng S, Hada M, Nakatsuji H (1996) Topology of density difference and force analysis. Theor Chim Acta 93:67–78
59. Li W, Zeng Y, Li X, Sun Z, Meng L (2016) Insight into the pseudo p-hole interactions in the $M_3H_6(NCF)n$ (M = C, Si, Ge, Sn, Pb; n = 1, 2, 3) complexes. Phys Chem Chem Phys 18:24672–24680
60. Lu B, Zhang X, Meng L, Zeng Y (2017) Insight into π-hole interactions containing the inorganic heterocyclic compounds S_2N_2/SN_2P_2. J Mol Model 23:233

Figures

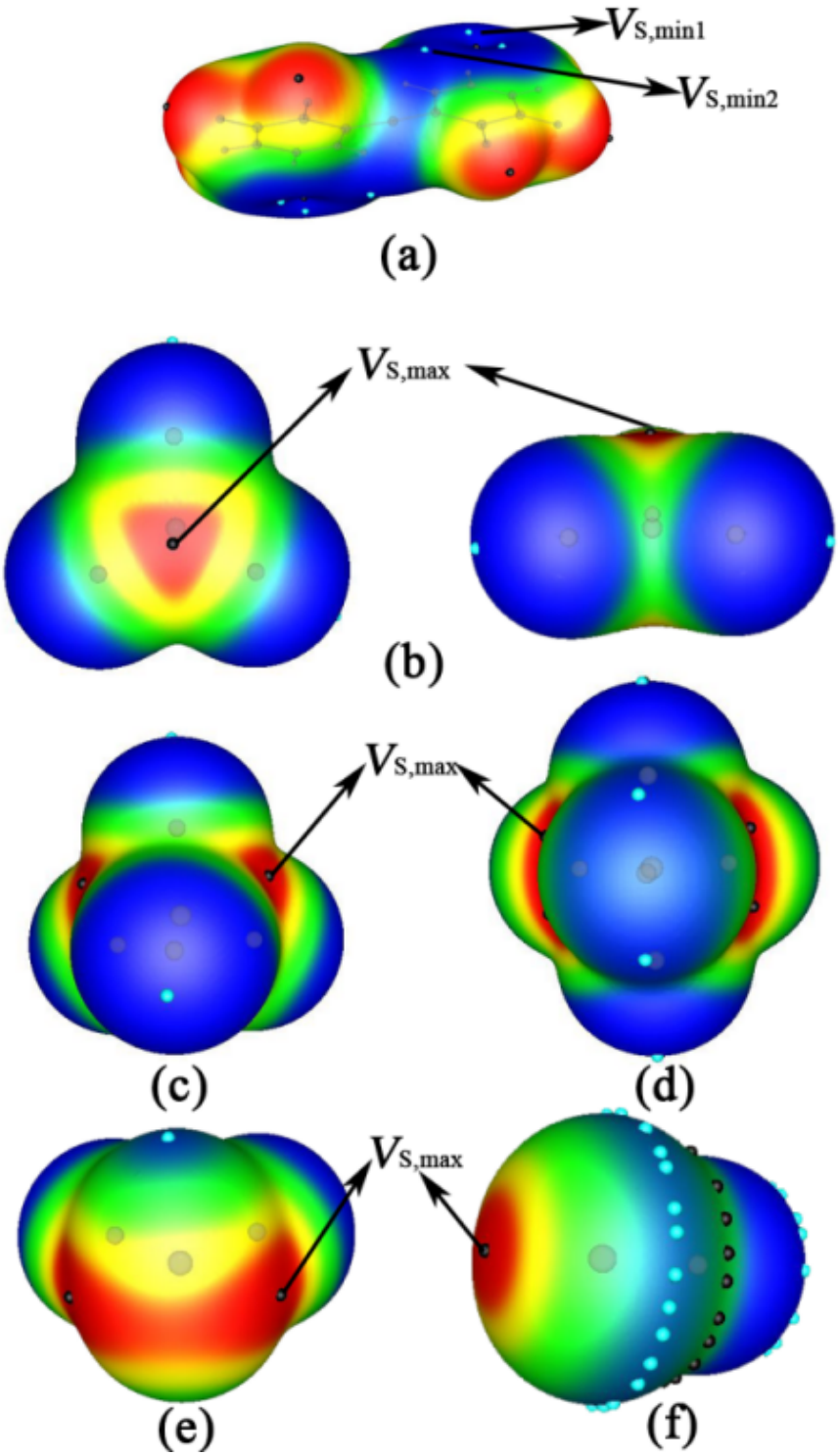

Figure 1

Contour maps of MEPs on the 0.001 au contour of the molecular electron density (a)DPC3, (b)AlF3, (c)SiF4, (d)PF5, (e)SF2, (f)ClF

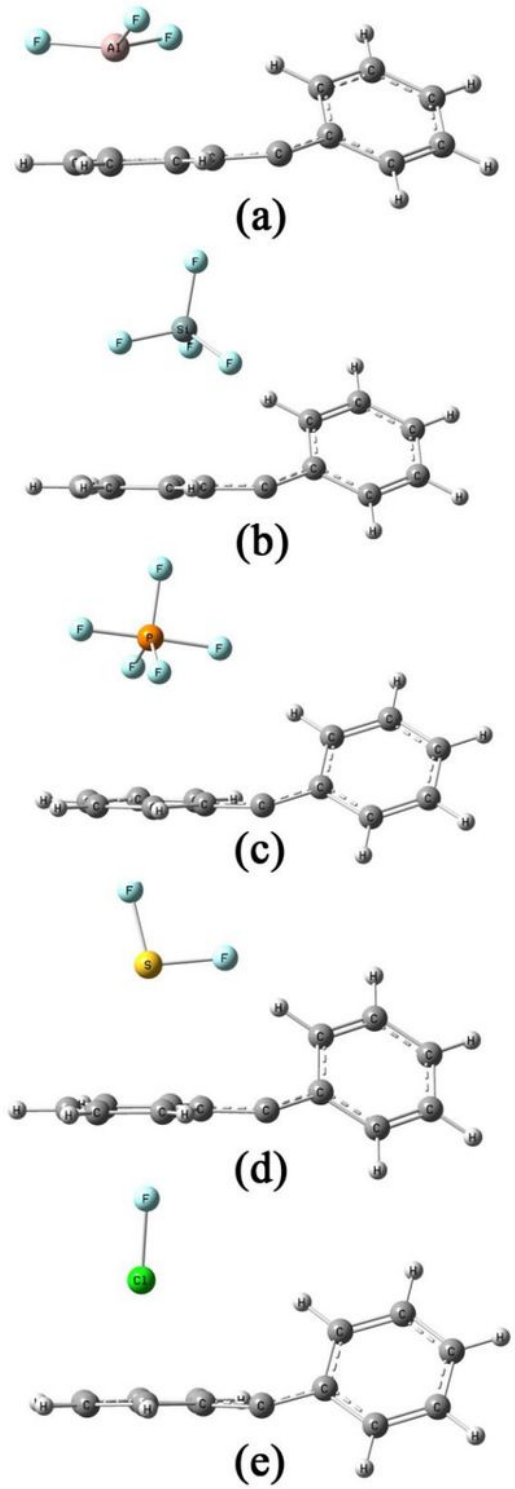

Figure 2

Optimized geometries of the complexes: (a) DPC3···AlF3; (b) DPC3···SiF4; (c) DPC3···PF5; (d) DPC3···SF2; (e) DPC3···ClF

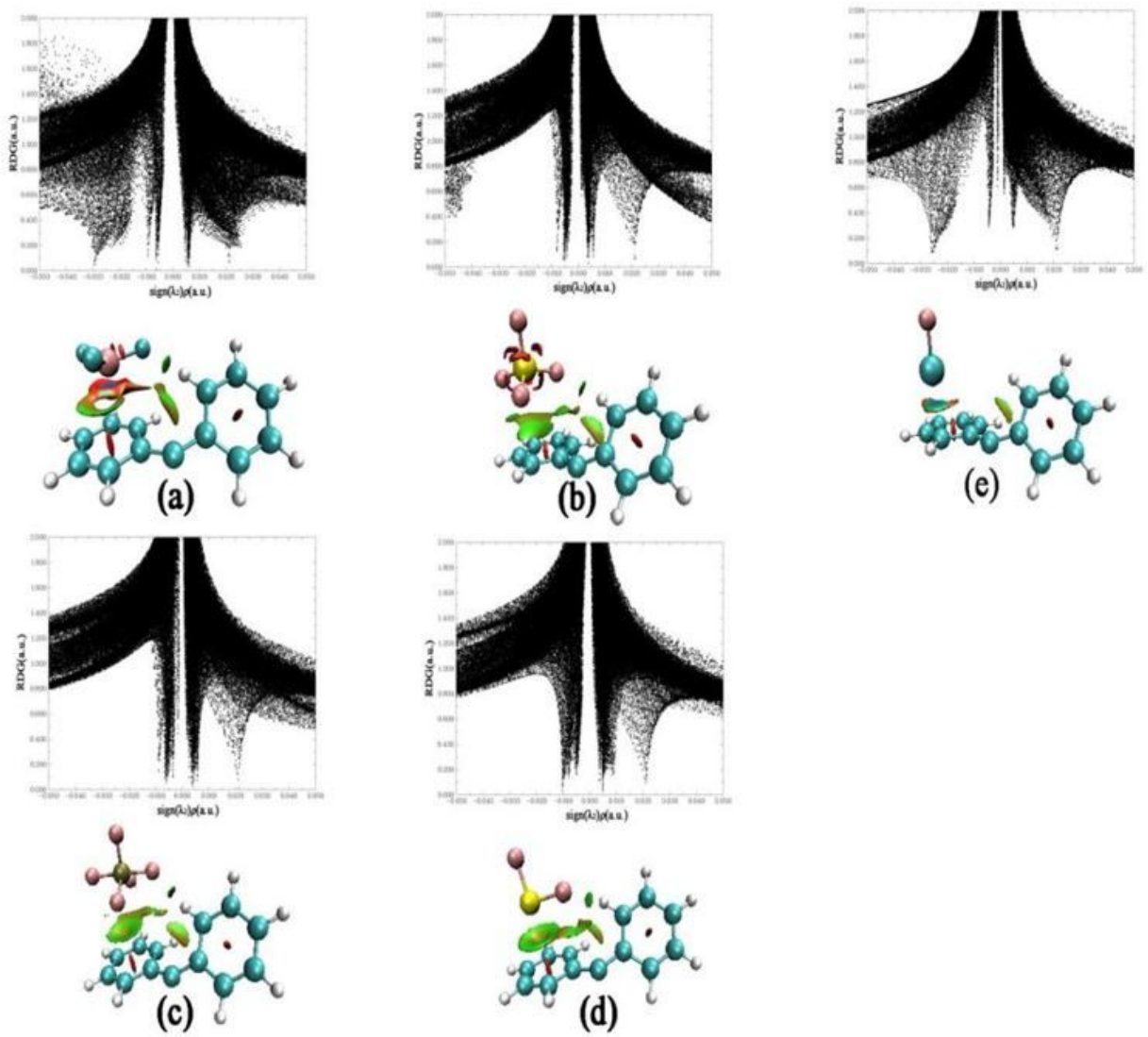

Figure 3

Plots of the reduced density gradient versus the electron density multiplied by the sign of the second Hessian eigenvalue (above) and gradient isosurfaces generated for s = 0.05 a.u (below) for complexes: (a)DPC3···AlF3, (b)DPC3···SiF4, (c)DPC3···PF5, (d)DPC3···SF2, (e)DPC3···ClF

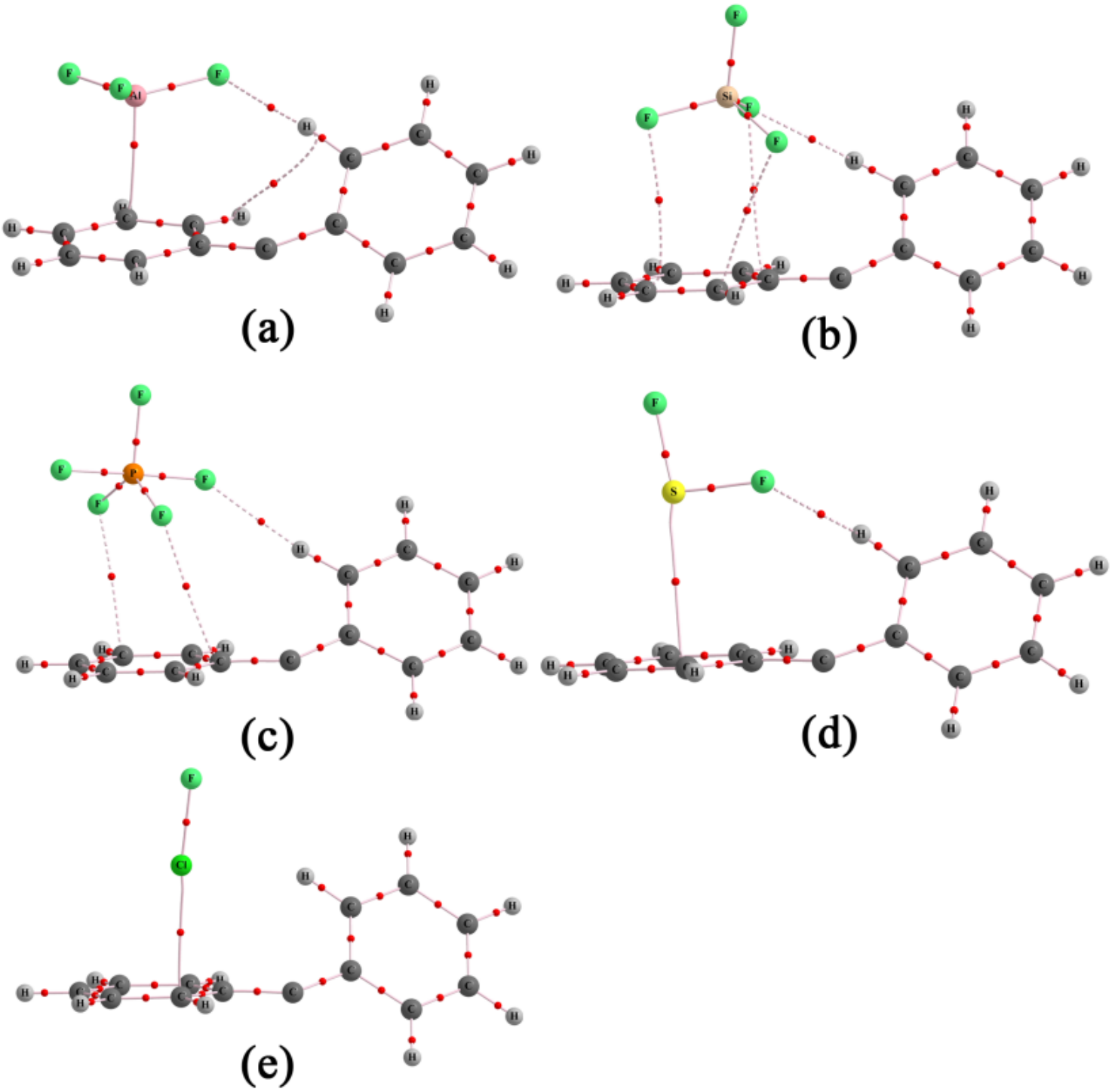

Figure 4

AIM molecular graphs of the complexes (a)DPC3···AlF3, (b)DPC3···SiF4, (c)DPC3···PF5, (d)DPC3···SF2, (e)DPC3···ClF

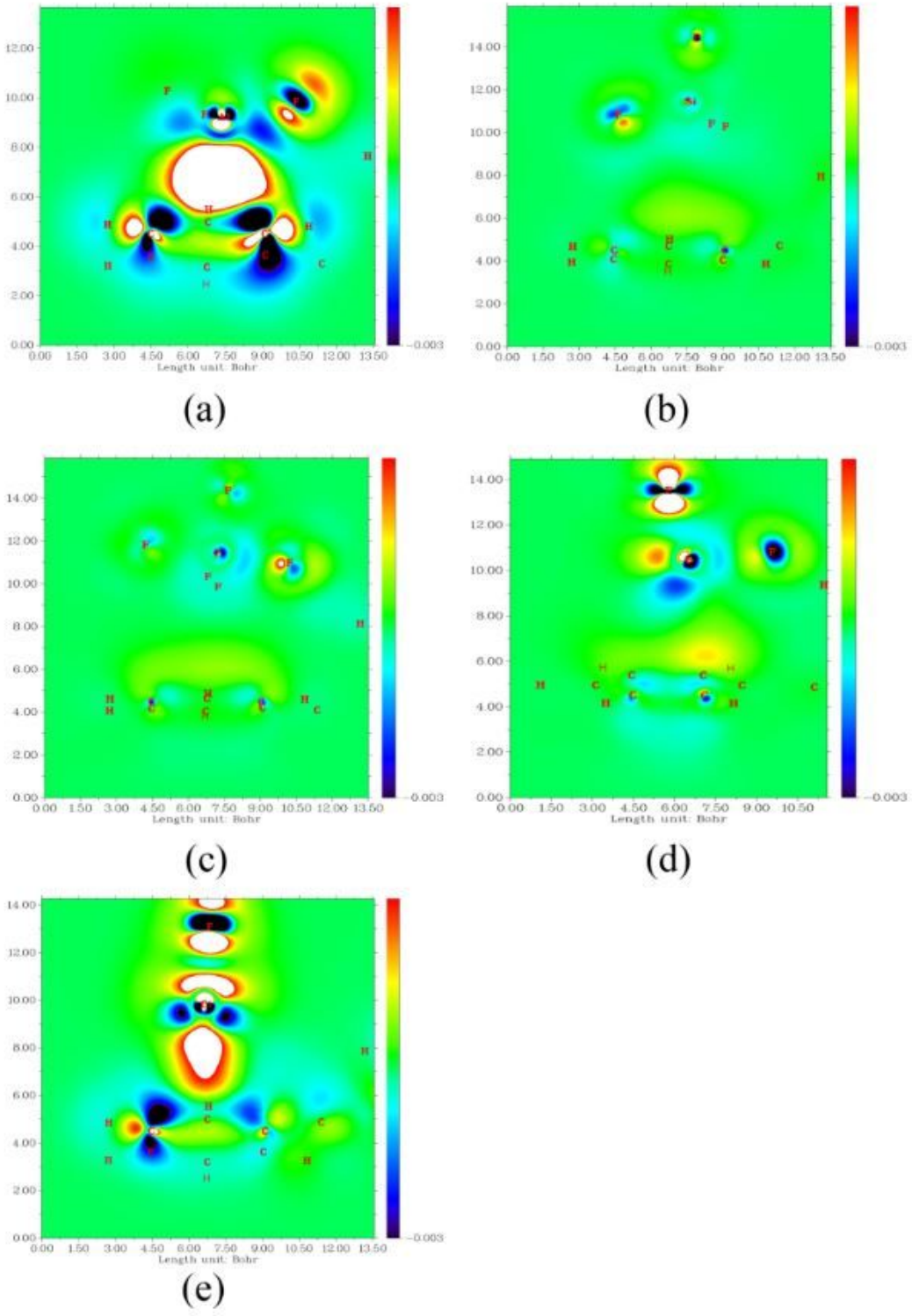

Figure 5

Computed density difference plots for the complexes (a)DPC3···AlF3, (b)DPC3···SiF4, (c)DPC3···PF5, (d)DPC3···SF2, (e)DPC3···ClF

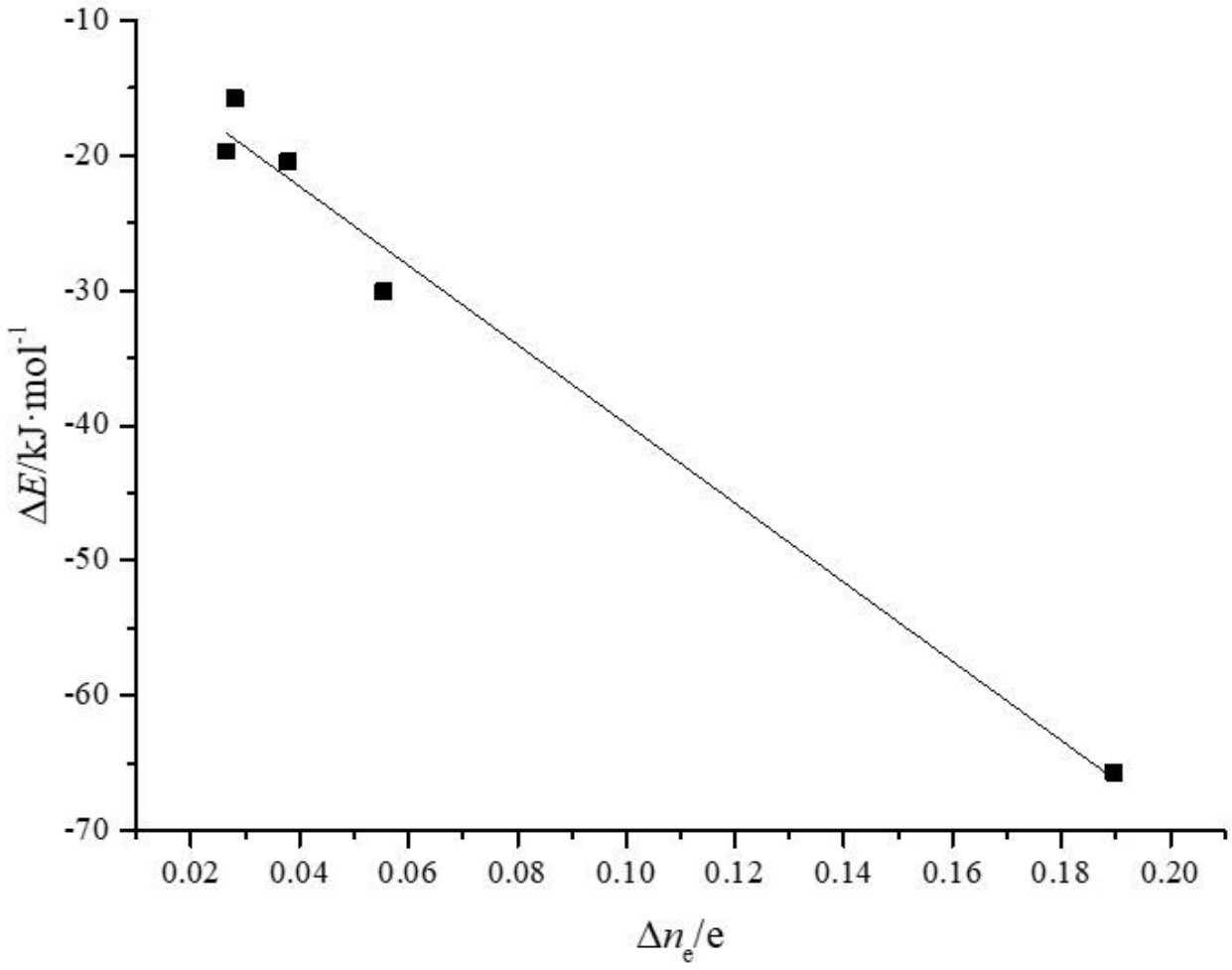

Figure 6

Liner correlation between the integral charge of the density difference region (Δne) and the binding energy (ΔE)

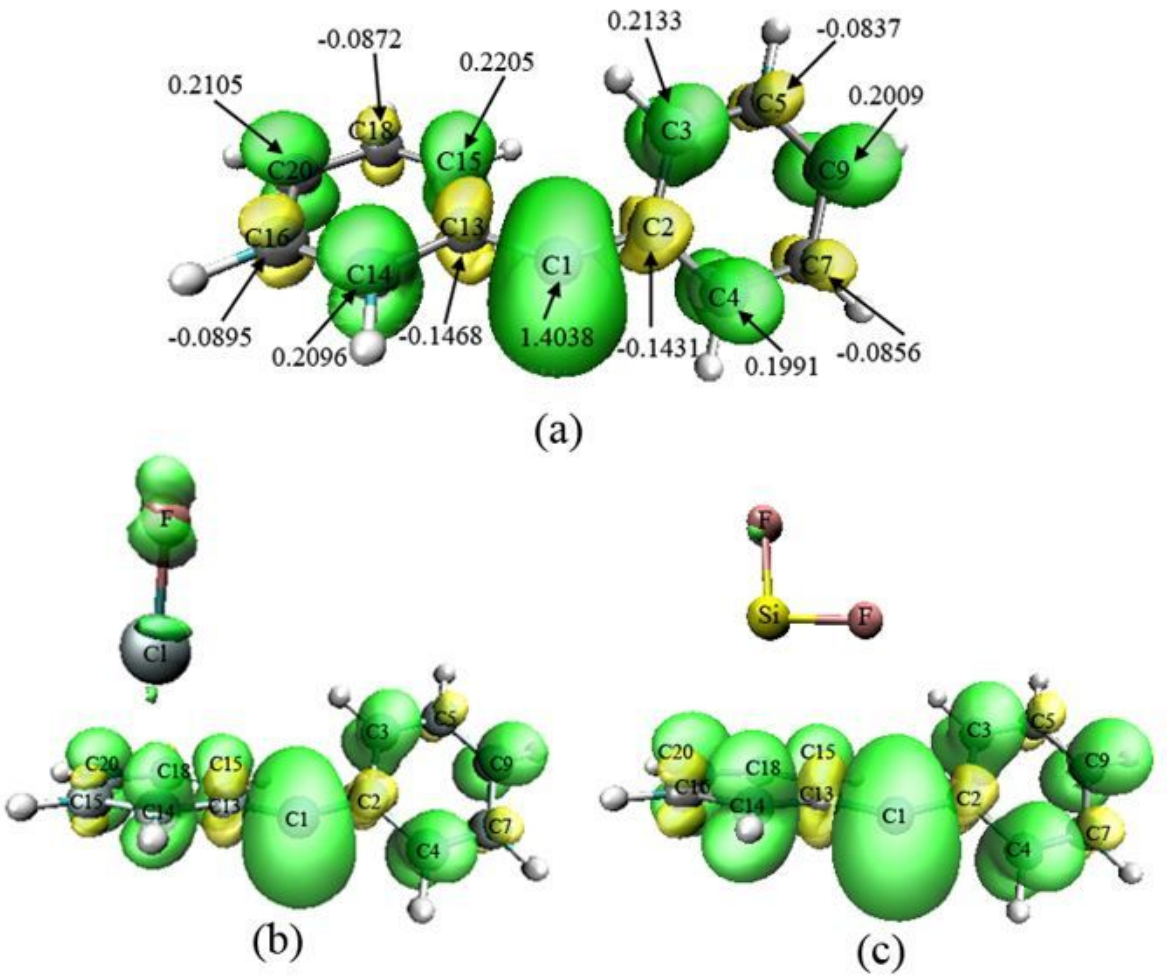

Figure 7

Maps of electron spin density for DPC3 and its complexes (a)DPC3, (b)DPC3···ClF, (c)DPC3···SF2